Proceedings of ICFDP7:
Seventh International Congress on Fluid Dynamics and Propulsion
December 18-20, 2001, Cairo, Egypt

ICFDP7-2001029

HEAT TRANSFER FOR LAMINAR FLOW IN INTERNALLY FINNED PIPES WITH DIFFERENT FIN HEIGHTS AND UNIFORM WALL TEMPERATURE

O. Zeitoun and A. S. Hegazy
Mech. Eng. Dept., King Saud University, P.O. box 800, 11421 Riyadh, Saudi Arabia

ABSTRACT
An analysis is presented for fully developed laminar convective heat transfer in a pipe provided with internal longitudinal fins, and with uniform outside wall temperature. The fins are arranged in two groups of different heights. The governing equations have been solved numerically to obtain the velocity and temperature distributions. The results obtained for different pipe-fins geometries show that the fin heights affect greatly flow and heat transfer characteristics. Reducing the height of one fin group decreases the friction coefficient significantly. At the same time Nusselt number decreases inappreciably so that such reduction is justified. The number of fins, at which maximum Nusselt number occurs, for different fin heights, is presented. This number lies between 6 and 12.

NOMENCLATURE
A_f dimensionless flow area of the finned pipe, Eq. (14)
a_f flow area of the finned pipe
C_p specific heat at constant pressure
f coefficient of friction, Eq. (12)
H dimensionless fin height h/r_o
h_1,h_2 fin heights
$\bar{h}$ average heat transfer coefficient at solid-fluid interface
KR fin conductance parameter, $\beta k_s/k_f$
k_f thermal conductivity of fluid
k_s thermal conductivity of fin
$\dot{m}$ mass flow rate
N number of fins
Nu Nusselt number, Eqs. (15) and (16)
P pressure
Q total heat transfer rate at solid fluid interface
Q_{f1},Q_{f2} heat tranfer rate at fin surface
q_f local heat flux at fin surface
q_u local heat flux at unfinned surface
q_w average heat flux at outer pipe-wall, $Q/(2\pi r_o l)$
R dimensionless radial coordinate r/r_o
Re Reynolds Number, Eq. (13)
r radial coordinate
r_o radius of pipe
r_1,r_2 radii of fin tips
T temperature
T_b bulk temperature
U dimensionless velocity
U_b dimensionless bulk velocity
u_z axial velocity
z axial coordinate
α angle between the flanks of two adjacent fins
β half the angle subtended by a fin
γ angle between the center-lines of two adjacent fins
θ angular coordinate
μ dynamic viscosity
ρ density
φ dimensionless temperature, Eq. (6)
φ_b dimensionless bulk temperature

INTRODUCTION
Internally finned pipes find wide applications in heat exchangers where an additional heat transfer area can be provided and thus heat transfer augmentation is obtained. The early analytical and experimental studies have been concerned with laminar flow and heat transfer in internally finned pipes of equal fin height [1-10]. The results of these studies have included the velocity distribution and friction factor, the temperature distribution and Nusselt number, and the influence of fin conductance on heat transfer characteristics.
The heat transfer effectiveness of internally finned pipes depends on different factors including fin conductance, the extension of the heat transfer surface between the solid and the fluid, and the local heat transfer coefficient. Each of these factors often depends on the others. For a given value of the thermal conductivity of the fin material, in order to enhance the conductance of the fins, it is necessary to increase the thickness and reduce the height. To increase the heat transfer surface, the extension of the fin must be augmented. The need to reduce the weight of internal finned pipe, in fact, has become even more important in heat exchangers. Therefore, the fin thickness must be reduced. The increase in the surface area of the fins results in elevating the friction factor, and consequently high power is required for pumping the fluid through the pipe.

The local heat transfer coefficient depends on the shape and the spacing of the fins in different ways. Many investigations [11-14] have been conducted to study the problem of optimizing the shape of the finned surfaces in order to increase heat transfer effectiveness and reduce the dimensions and the weight of
internally finned pipe. These investigations resulted in finding out the profiles, which maximize the heat transfer per unit of finned pipe length or surface. However, such profiles seem to be too complicated to manufacture. Moreover, nothing about coefficient of friction has been published, which is anticipated to be relatively high.
Improvements in the local heat transfer coefficient can be obtained by altering the velocity pattern between the fins. If the fins inside the pipe are of different heights the velocity pattern between them will change. The present paper is intended to examine the effect of using fins of different heights on heat transfer in internally finned pipes. Therefore, this paper presents an analysis for fully developed laminar convective heat transfer of Newtonian fluid in pipes provided with two groups of internal fins. These two groups have different fin height. The fins are arranged in such a way that each two consecutive fins are of different heights. Therefore the number of fins should be even.

ANALYSIS

Figure 1 shows the flow domain of the internally finned pipe to be studied in the current paper. The pipe has an inner radius r_o. The tips of the fins lie on two circular arcs with radii r_1 and r_2, concentric with the center line of the pipe. The fins are straight and uniformly distributed around the periphery of the pipe cross section. Due to the geometrical symmetry of the flow domain as shown in Fig. 1, solution for the governing equation is sought only between the axes of two consecutive fins; i.e. between $\theta = 0$ and $\theta = \gamma$. The flow is assumed to be steady, laminar and fully developed. Moreover it is assumed that the fluid is Newtonian and has uniform properties and the viscous dissipation within the fluid is neglected. Under these assumptions the momentum equation reduces to:

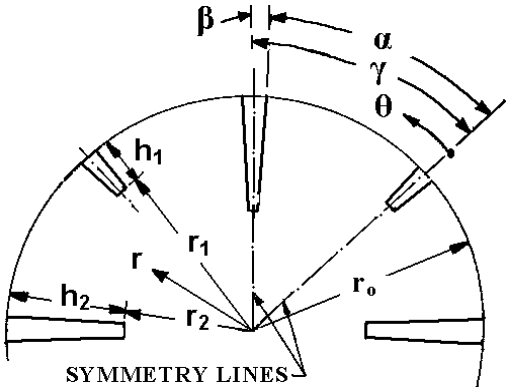

Fig. 1. Flow field geometry

$$\frac{1}{r}\frac{\partial}{\partial r}\left(r\frac{\partial u_z}{\partial r}\right)+\frac{1}{r^2}\frac{\partial^2 u_z}{\partial \theta^2}=\frac{1}{\mu}\frac{dp}{dz} \tag{1}$$

Using dimensionless variables

$$R=\frac{r}{r_o} \quad \text{and} \quad U=\frac{u_z}{\frac{r_o^2}{\mu}\left(-\frac{dp}{dz}\right)} \tag{2}$$

Eq. (1) can be written in a dimensionless form as:

$$\frac{1}{R}\frac{\partial}{\partial R}\left(R\frac{\partial U}{\partial R}\right)+\frac{1}{R^2}\frac{\partial^2 U}{\partial \theta^2}=-1 \tag{3}$$

The boundary conditions for the fluid flow domain are:

$$\text{at } R=1,\ \beta \le \theta \le \alpha : U=0 \tag{4a}$$
$$\text{at } R_2 \le R \le 1,\ \theta=\beta : U=0 \tag{4b}$$
$$\text{at } R_1 \le R \le 1,\ \theta=\alpha : U=0 \tag{4c}$$
$$\text{at } 0 \le R \le R_2,\ \theta=0 : \frac{\partial U}{\partial \theta}=0 \tag{4d}$$
$$\text{at } 0 \le R \le R_1;\ \theta=\gamma : \frac{\partial U}{\partial \theta}=0 \tag{4e}$$
$$\text{at } R=0 \text{ for all values of } \theta : \frac{\partial U}{\partial R}=0 \tag{4f}$$

For a fully developed temperature profile and negligible axial conduction, the energy equation can be reduced to:

$$\frac{1}{r}\frac{\partial}{\partial r}\left(r\frac{\partial T}{\partial r}\right)+\left(\frac{1}{r^2}\frac{\partial^2 T}{\partial \theta^2}\right)=\frac{\rho C_p}{k_f}u_z\frac{\partial T}{\partial z} \tag{5}$$

The axially invariant temperature profile can be written in terms of dimensionless temperature as:

$$\varphi(r,\theta)=\frac{T_{(z,r,\theta)}-T_w}{q_w(z)\,r_o/k_f} \tag{6}$$

Using the dimensionless variables given by Eqs. (2) and (6) Eq. (5) can be written in the following dimensionless form:

$$\frac{\partial}{\partial R}\left(R\frac{\partial \varphi}{\partial R}\right)+\frac{1}{R}\frac{\partial^2 \varphi}{\partial \theta^2}=\frac{2\pi R}{A_f}\frac{U}{U_b}\frac{\varphi}{\varphi_b} \tag{7}$$

where A_f is the dimensionless flow area expressed as:

$$A_f=a_f/r_o^2=\pi-\frac{N\beta}{2}\left(2-R_1^2-R_2^2\right) \tag{8}$$

In a similar way, the conduction equation within the fins in a dimensionless form can be written as:

$$\frac{\partial}{\partial R}\left(R\frac{\partial \varphi}{\partial R}\right)+\frac{1}{R}\frac{\partial^2 \varphi}{\partial \theta^2}=0 \tag{9}$$

The appropriate boundary conditions for Eqs. (8) and (9) are:

$$\text{at } R=1,\quad 0 \le \theta \le \gamma : \phi=0 \tag{10a}$$
$$\text{at } \theta=0 \text{ for all } R : \frac{\partial \varphi}{\partial \theta}=0 \tag{10b}$$
$$\text{at } \theta=\gamma \text{ for all } R : \frac{\partial \varphi}{\partial \theta}=0 \tag{10c}$$
$$\text{at } R=0 \text{ for all } \theta : \frac{\partial \varphi}{\partial R}=0 \tag{10d}$$

COMPUTATIONAL PROCEDURE

The differential equations (3), (7), and (9) subjected to the boundary conditions given by equations (4) and (10) were solved numerically using the finite volume method. Details

of this method are given in Patankar [15]. A 31 x 37 (radial r x angular θ) grid was employed in the calculation domain. The grid spacing in θ - direction was chosen to be finer in and near the fin wall ($\delta\theta \leq 0.02$ rad.). In the r-direction, the grid spacing was finer close to both the pipe wall and the fins lower tips ($\delta R \leq 0.02$). Exploratory computations on finer grids were conducted for different fin-pipe geometries and the resulting changes in both velocity and temperature values were too small to justify the increased computation time.

The discretized equations were obtained by integrating Eqs. (3), (7), and (9) over the domain of control volumes. These equations were solved by iteration until a converged solution is obtained where the change in velocity for Eq. (3) and temperature for Eq. (7) and (9) at any point in the domain is less than 10^{-7} of its value in a previous iteration step. The velocity profile obtained by solving Eq. (3) is used as input to the Eq. (7). The dimensionless bulk velocity U_b and temperature φ_b were calculated using Simpson's rule. This computational technique was tested by prediction of the well known cases of laminar flow through finless pipes [16]. The results of velocity and temperature profiles showed a deviation less than 0.5%, while the coefficient of friction results showed a maximum deviation in f.Re of 0.08% and the Nusselt number results indicated a maximum error of 0.44%.

To be able to reveal the effect of unequal heights of the fins on the fluid flow and convective heat transfer in internally finned pipes, the following range of computation were covered:

$$4 \leq N \leq 16, \quad (11a)$$
$$\leq H_1 \leq 0.8, \quad (11b)$$
$$\leq H_2 \leq 0.8, \quad (11c)$$
$$\text{and} \quad \beta = 3 \text{ degrees} \quad (11d)$$

The single value of β represents a typical value for internally finned pipes already manufactured and tested [1].

To verify the numerical accuracy of the solution procedure, numerical results were first obtained for the case of equal fin heights ($H_1=H_2$) and compared with those reported in [3]. The agreement was very good and the plots of the two results for both velocity and temperature profiles were hardly distinguishable.

RESULTS AND DISCUSSION

For smooth pipe with radius r_o, the coefficient of friction f and Reynolds number Re are normally defined as :

$$f = \left(\frac{4 r_o \rho a_f^2}{\dot{m}^2} \right) \left(- \frac{dP}{dz} \right) \quad (12)$$

and

$$Re = \frac{2 r_o \dot{m}}{\mu a_f} \quad (13)$$

Eqs. (12) and (13) have been used for correlating the coefficient of friction results of internally finned pipes because they provide a basis for comparison with smooth pipes. The product f.Re can be placed in the following dimensionless form:

$$f.Re = \frac{8}{U_b} \quad (14)$$

Computations for determining the distribution of fluid flow velocity as well as temperature of both the fluid and fins were carried out, for a wide range of internally finned pipe geometries. Selected samples for dimensionless velocity profiles U/U_b are shown in Figure 2. The diagrams of this figure show clearly that for $H_1 = 0.8$ closed loops of iso-velocity lines exist in the space between each two consecutive fins. These loops diminishes gradually as H_1 gets smaller. Such loops represent an important feature of the flow in internally finned pipes, since they affect the temperature distribution and hence the rate of heat transfer from or into the pipes. The existence of these loops has been investigated in the present study. It has been found that they occur for the values of H_1 and H_2 greater than 0.5. If any of these two dimensionless parameters or both become less than 0.5 the loops disappear completely.

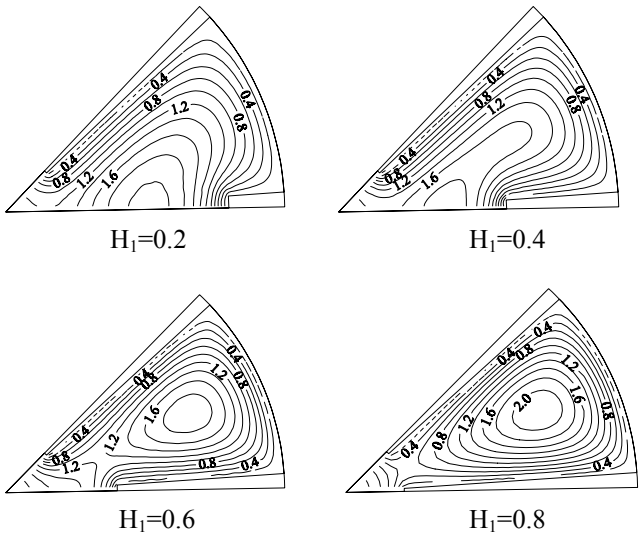

Fig. 2. Iso-velocity lines U/U_b, N=8

Based on Eq. (14), the average coefficient of friction has been determined. Samples of the results are shown in Figures 3a, 3b and 3c for $H_2 = 0.4$, 0.6 and 0.8, respectively. In these figures the product f.Re is plotted versus the number of fins N. It is seen from Fig. 3 that the coefficient of friction grows steeply in all cases as the number of fins is increased. Both H_1 and H_2 affect greatly the value of the coefficient of friction f. It grows fast as H_1 and H_2 are increased. However, keeping the value of one of them high and decreasing the other results in considerable decrease in f.Re.

Samples of the isotherms (constant dimensionless temperature $T-T_w/T_b-T_w$ lines) over the whole domain are displayed in Figure 4. Examining the isotherms in Fig. 4, it can be concluded that, at $H_1=H_2=0.8$ closed loops exist. Keeping $H_2=0.8$, the loops diminishes gradually as H_1 decreases. In general the investigation of the existence of these loops has revealed that they disappear as long as the value of H_1 and H_2 or one of them is less than 0.6.

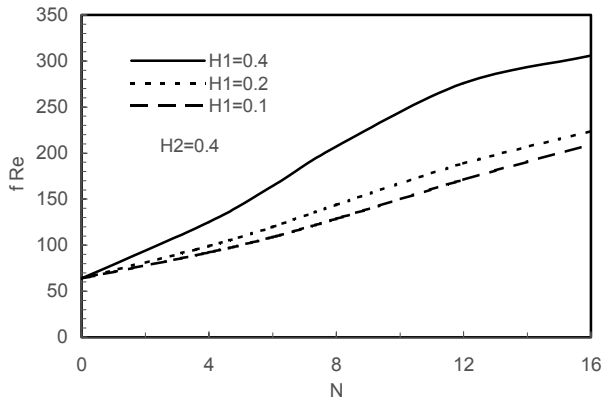

Figure 3a. Effect of fins number on coefficient of friction

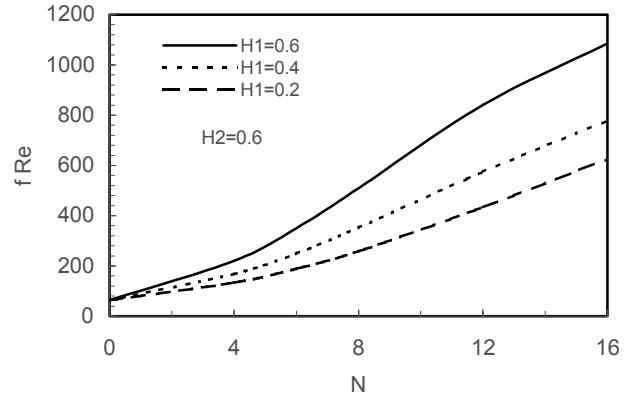

Fig. 3b. Effect of fins number on coefficient of friction

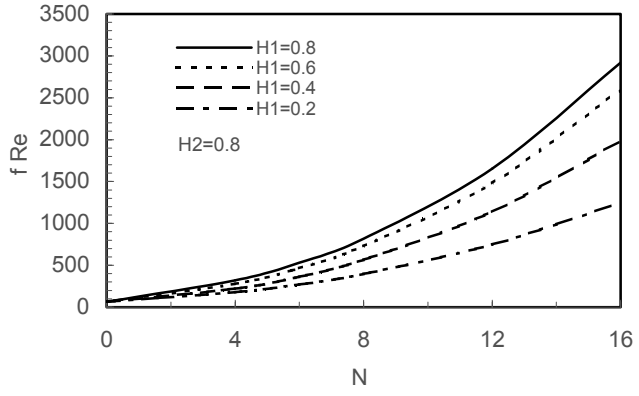

Fig. 3c. Effect of fins number on coefficient of friction

Variation of ratio q_u/q_w of local heat flux on the tube unfinned surface and the average heat flux at solid fluid interface along the tube surface confined between two consecutive fins is illustrated in Figure 5. It is obvious from this figure that, for equal fin heights, q_u/q_w has a maximum value midway between the two fins. As H_1 decreases q_u/q_w recedes in the region near the higher fin while it increases in the vicinity of the shorter one and its maximum is shifted towards the higher fin till it occurs quite close to the higher fin at H_1=0.3. Further decrease in H_1 results in shifting the maximum q_u/q_w towards the shorter fin. Naturally it would have its maximum in place of the shorter fin as the latest vanishes (i.e. H_1=0).

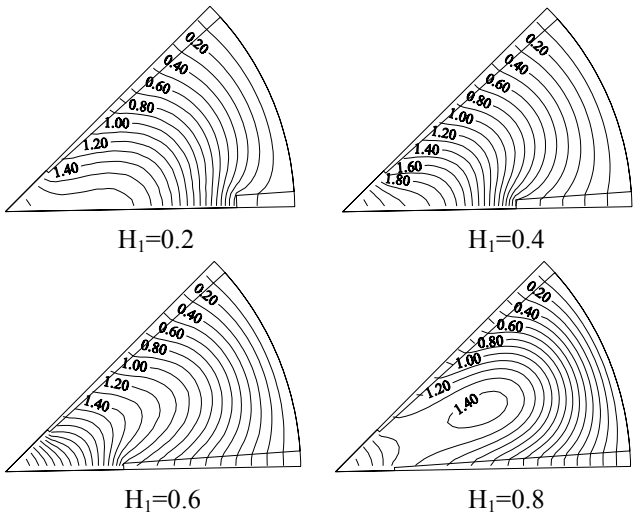

Fig. 4. Isotherms $(T_w-T)/(T_w-T_b)$, N=8, H2=0.8, KR=1.0

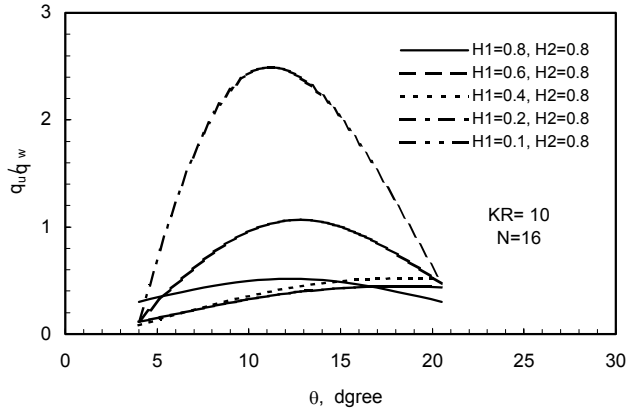

Fig. 5. Variation of heat flux on the unfinned surface

The heat flux ratio q_f/q_w along the fin height of the longer fin and of the shorter one is shown in Figures 6a and 6b, respectively. To comprehend the results of Figs. 6a and 6b, we have to consider the velocity and temperature around the fins (see Figs 2 and 4). For long fin height H_1 the fluid velocity at the fins bases is very small resulting in small heat transfer coefficients and consequently small heat flux is transferred to the colder fluid bulk. As we move along the fin towards the tip, increasing velocities are encountered which result in increasing heat flux with maximum at the tips of the fins. As H_1 becomes shorter, H1<0.5, the closed isovelocity loops (Fig. 2) disappear and fluid velocity increases in the region between the tips of the two fins. This leads to increase the coefficient of heat transfer and consequently the heat flux in this region. Therefore the heat flux is enhanced near the middle of the long fin and at the tip of the short one.

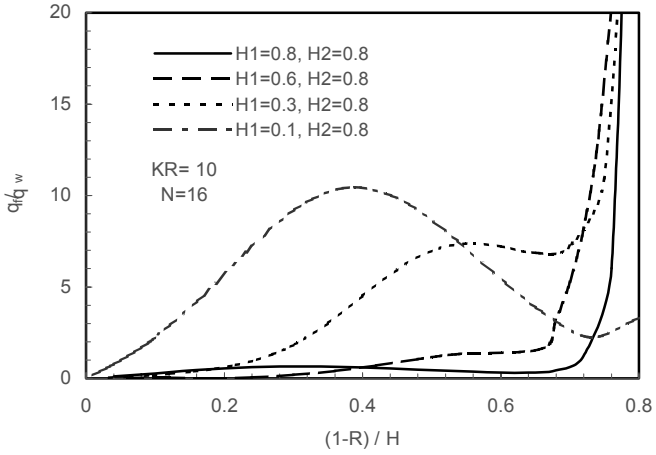

Fig. 6a. Heat flux distribution on the surface of the longer fin

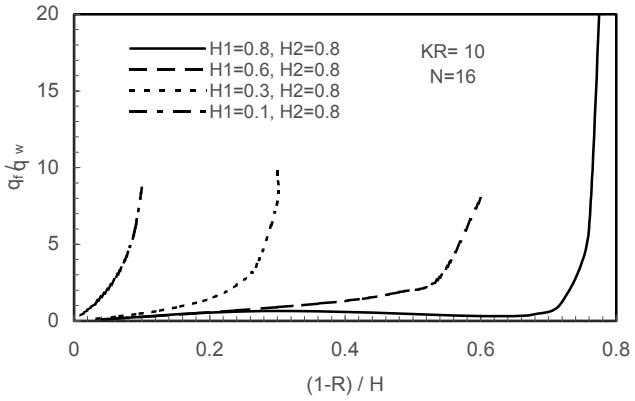

Fig. 6b. Heat flux distribution on the surface of the shorter fin

The ratio Q_f/Q of heat transfer rate by each fin and the heat transfer rate at solid fluid interface (i.e. surface of both fins and unfinned tube wall confined between the two fins) is plotted in Figure 7 versus dimensionless fin height H_1 for N=16, and KR=10. It is clear from this figure that, when the two fins have equal heights they contribute equally to heat transfer (i.e. $Q_{f1}/Q = Q_{f2}/Q$). As the height of one fin gets shorter, its effect on heat transfer is reduced while the the effect of the longer fin is enhanced. It is also obvious from Fig. 7 that the sum of Q_{f1}/Q and Q_{f2}/Q is almost constant. The effect of the shorter fin on heat transfer almost vanishes as the ratio of H_1/H_2 becomes less than Ca. 0.55. One can see clearly from this figure that the heat transfer between the fluid and solid surface is almost brought about by the surface of the fins and the unfinned solid surface of the pipe contribute inconsiderably to this process.

The parameter which is commonly used as a measure of any heat transfer surface is the Nusselt Number is defined as:

$$Nu = \frac{\bar{h}(2\,r_o)}{k_f}, \qquad \text{where} \qquad \bar{h} = \frac{q_w}{T_w - T_b}$$

From which it follows:

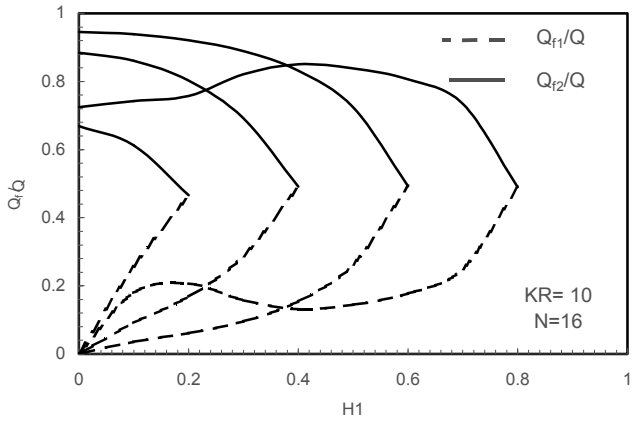

Fig. 7. Ratio of heat transfer rate at each fin surface and total heat transfer rate at solid-fluid surface

$$Nu = \frac{2\,r_o\,q_w}{k_f\,(T_w - T_b)} \tag{15}$$

and in dimensionless form:

$$Nu = \frac{2}{\varphi_b} \tag{16}$$

The value of Nusselt Number given by Eq. (16) can be used for comparing different fine-pipe geometries in enhancing heat transfer. Samles of the obtained Nuselt number are shown in Figs. 8 through 9.

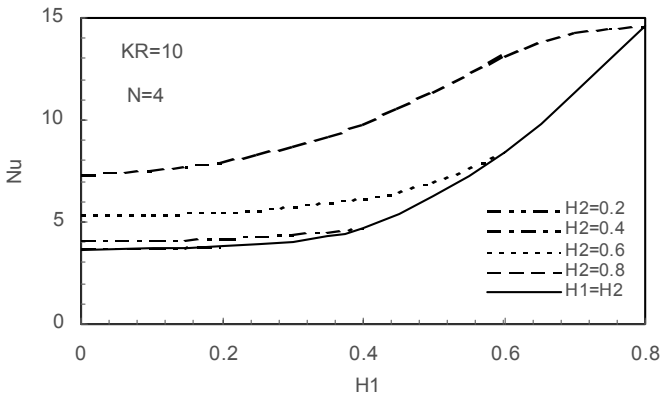

Fig. 8a. Effect of heights of fins on Nusselt number

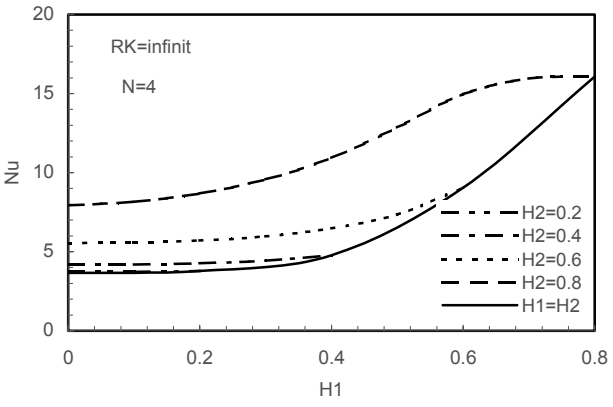

Fig. 8b. Effect of heights of fins on Nusselt number

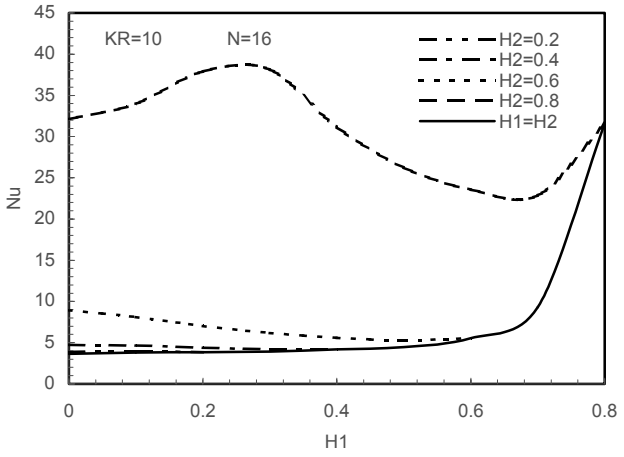

Fig. 8c. Effect of heights of fins on Nusselt number

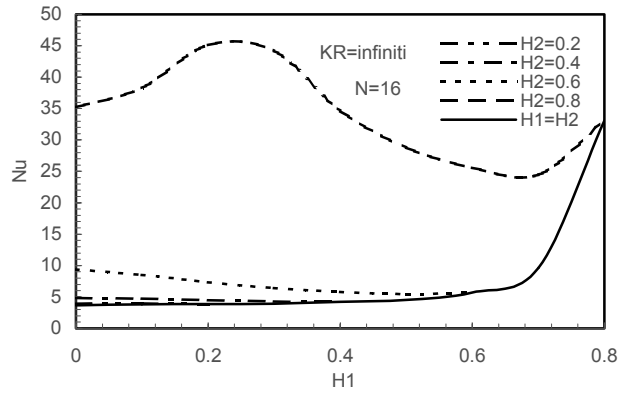

Fig. 8d. Effect of heights of fins on Nusselt number

In Figure 8, Nusselt number Nu is plotted versus the height ratio H_1 for H_2=0.2 0.4, 0.6, 0.8 and H_2=H_1. As can be seen from the diagrams of Fig. 8, Nu is increased at low fin numbers (N=4) with increasing H_1 and H_2 as well, and reaches its maximum at H_2=H_1. Nu is remarkably enhanced as H_2 gets higher. As for large numbers of fins (N=16), Nu is less for a specific value of H_2 (in the range H_2<0.7) as H_1 grows. Reffering to Figs. 3, it is clear that the coefficient of friction gets higher in the above mentioned range as with increasing H_1. Therefore, it is not worth selecting fins of different heights and instead of that half the number of fins is to be used. For the range of H_2>0.7, Nu is enhanced with growing values of H_1 till it reaches its maximum at a small value of H_1 (e.g. maximum Nu for H_2=0.8 occurs at H_1=0.3). Further increase in H_1 leads to a considerable reduction in Nu till a minimum and then it grows again till H_1=H_2, and even so it is still less than the maximum value. Referring again to Figs. 3, it can concluded that the coefficient of friction for higher values of H_2 and low values of H_1 is relatively low justified by the enhanced heat transfer through the high values of Nu. The diagrams of Fig. 8 shows also clearly that Nu is improved by increasing KR due to the enhanced heat transfer by conduction through the fins. However, this improvement is appreciable only for high values of H_1 and H_2.

Figure 9 displays the effect of fins number on the Nusselt number. It is evident from the diagrams of Fig. 8 that the number of fins at which maximum Nu is obtained depends on the values of both H_2 and H_1. For H_2=0.8 the maximum Nu is obtained when N=12 irrespective of the value of H_1. For H_2=0.6 the maximum Nu occurs at N=6 when H_1>0.5 whereas for H_1<0.5, the number of fins at which maximum Nu occurs, is 12.

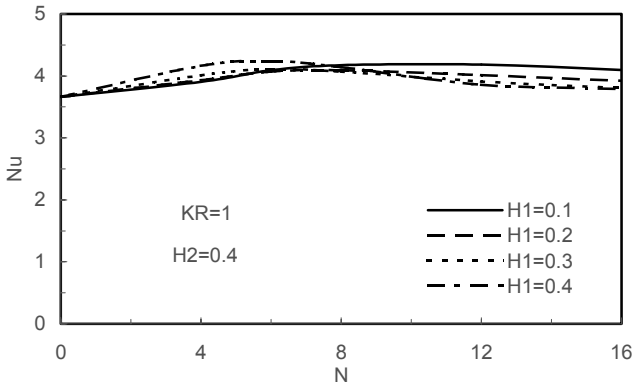

Fig. 9a. Dependence of Nusselt number on fins number

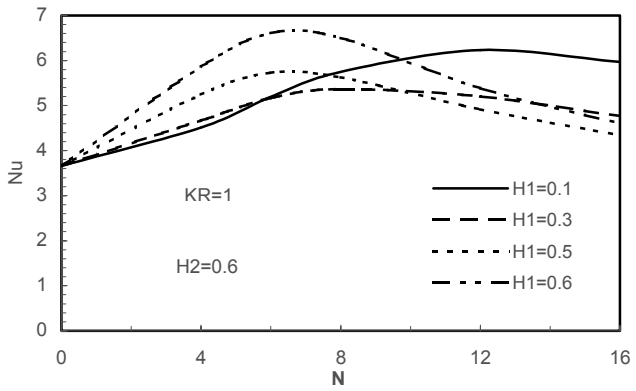

Fig. 9b. Dependence of Nusselt number on fins number

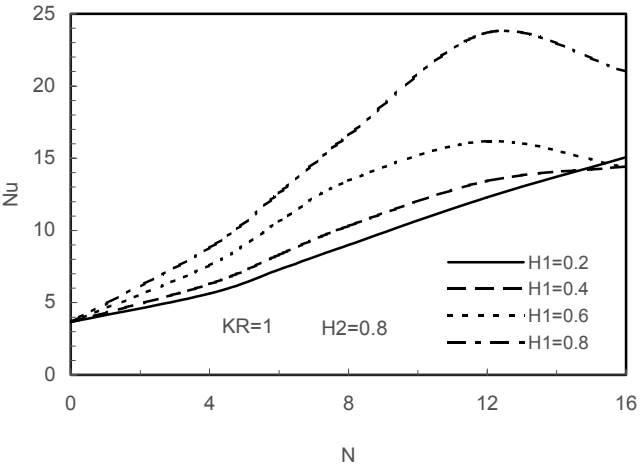

Fig. 9c. Dependence of Nusselt number on fins number

CONCLUSIONS

From the previous analysis and discussion the following conclusions can be drawn for pipes provided with two groups of internal fins having different heights.

1. Coefficient of friction increases as the number of fins and fins heights are increased. However, the coefficient of friction is considerably reduced as the height of one group of the fins gets shorter.
2. Heat transfer in internally finned pipe in mainly caused by the surfaces of the fins, especially when the heights of the fins are long. The contribution of the unfinned surface of the pipes is very small compared with that of the fins surfaces.
3. Nu has its maximum values when the two groups of fins are equal in height for low number of fins. In contrast for large numbers of fins Nu has its highest value at very small height of the shorter fins when the ratio of the height of the longer fin and the radius of the pipe is less than 0.7. For greater values of this ratio, the Nu is maximal at short height of the shorter fins and in this case the coefficient of friction is relatively low.
4. The number of fins at which maximum Nusselt number is obtained, is 6 for short fins and 12 for long fins.

REFERENCES

1. Watkinson, A. P.; . Miletti, P. L; Kubanek, G. R., 1975, "Heat Transfer and Pressure Drop of Internally Finned Tubes in Laminar Oil Flow" . *ASME Paper 75-HT-41.*
2. Mamer, W. J. ; Bergles, A. E., 1978, "Augmentation of Tube-Side Laminar Flow Heat Transfer by Means of Twisted Tape Inserts, Static Mixer Inserts and Internally Finned Tubes", *J. Heat Transfer 1978,* Hemisphere, Washington, Vol. 2,.
3. Soliman, H. M., Chau, T. S. ; Tnupp, A. C., 1980 "Analysis of Laminar Heat Transfer in Internally Finned Tubes with Uniform Outside Wall Temperature", *J. Heat Transfer,* Vol. 102, pp. 598-604.
4. Soliman, H. M., 1979, "The Effect of Fin Material on Laminar Heat Transfer Characteristics of Internally Finned Tubes", *Advances in Enhanced Heat Transfer,* ed. J. M. Chenoweth, J. Kaeilis, J. W. Michel, and S. Shenkman, Book No. 100122. ASME, New York.
5. Soliman, H. M.; Feingold, A., 1977, "Analysis of Fully Developed Laminar Flow in Longitudinally Internally Finned Tubes", *Chem. Eng. J.,* Vol. 14,.
6. Bergles, A. E.; Joshi, S. D., 1983, "Augmentation Techniques for Low Reynolds Number In-Tube Flow", *Low Reynolds Number Flow in Heat Exchangers,* S. Kakac, R. K. Shah, and A. E. Bergles, Hemisphere, Washington.
7. Masliyah, J. H.; Nandakakumar, K., 1976, "Heat Transfer in Internally Finned Tubes", ASME Journal of Heat Transfer 98.
8. Nandakakumar, K., Masliyah, J. H., 1975, "Fully Developed Viscous Flow in Internally Finned Tubes"., The chemical Engineering Journal 10.
9. Huq, M.; Aziz-ul Huq, A. M.; Rahman, M. M., Juli 1998, "Experimental Measurements of Heat Transfer in an Internally Finned Tube. International Communication in Heat and Mass Transfer.
10. Soliman, H. M.; Feingold, A. 1978, "Analysis of Heat Transfer in Internally Finned Tubes Under Laminar Flow Conditions", Proceedings of the sixth International Heat Transfer Conference, Vol. 2.
11. Tsukamoto, Y.; Seguchi, Y., 1984, "Shape Optimization Problem for Minimum Volume Fin, Heat Transfer Japanese Research 13.
12. Fabbri, G., 1997, "A Genetic Algorithm for Fin Profile Optimization, Int. J. Heat and Mass Transfer 40 (9).
13. Fabbri, G., 1998, "Heat Transfer Optimization in Internally Finned Tubes under Laminar Flow Conditions", Int. J. Heat and Mass Transfer 41 (10).
14. Lorenzini, E.; Spiga, M.; Fabbri, G., 1994, "A Polynomial Fin Profile Optimization", Int. J. Heat and Technology 12.
15. Patanker, S. V., 1980, Numerical Heat Transfer and Fluid Flow, McGraw Hill.
16. Incoropera, F. P., Dewitt, D., 1990, Introduction to Heat Transfer, John Wiley.